Analysis of Time Series of Satellite Passive Microwave Observations of Snow over the Colorado Cold Lands Processes Experiment Study Region

R.E.J. KELLY[1] AND T. MARKUS[2]

ABSTRACT

Several passive microwave remote sensing approaches have been developed to estimate snow water equivalent (SWE). Methods range from static empirically-calibrated models, to complex radiative transfer models with several variants between these end-members. Most approaches are based on instantaneous observations of brightness temperature (TBs) of the snow which are caused by snow and non-snow surface emissivity and physical temperatures. Significant short-term (e.g. day–to-day) temporal variability is often observed in SWE estimates even though it is unlikely that SWE varies over short-term scales. Recent work by Markus et al. (2006) has shown that atmospheric affects can adversely affect the estimation capability of passive microwave algorithm estimates of SWE and work by others has demonstrated that snowpack physical properties also control the microwave emission. This paper analyses the time series of brightness temperatures from the Advanced Microwave Scanning Radiometer – EOS (AMSR-E) channels through the winter season of 2002-2003 during the Cold Lands Processes Experiment (CLPX) in Colorado to better understand the variability found in the data. *In situ* surface air temperatures from CLPX show strong correlation with the 10 and 18 GHz AMSR-E Tbs and a weaker correlation with 36 GHz Tb observations suggesting that the unaccounted-for contribution of air temperature to the 18 and 36 GHz emission is a likely cause of the estimated variation in microwave scattering from day-to-day. If this thermal signal can be removed, algorithms can represent more effectively snow emissivity which is directly related to snow water equivalent.

Keywords: snow; AMSR-E; hydrology; remote sensing; microwave

INTRODUCTION

The upwelling radiation observed as the apparent temperature at a satellite microwave radiometer (*Tb*) can be expressed as:

$$Tb = e_s T_s e^{-\tau} + Tb_{up} + (1-e_s) Tb_{down}\ e^{-\tau} + (1-e_s) Tb_{cosmic}\, e^{-2\tau} \quad (1)$$

where e_s is the emissivity of the Earth surface, T_s is the surface physical temperature, $e^{-\tau}$ is the atmospheric transmissivity, Tb_{down} is the re-reflected downward atmospheric emission and Tb_{cosmic} is the reflected cosmic radiation with a two-way transmission path. In general the atmospheric emission components (Tb_{up}, Tb_{down} and Tb_{sp}) are neglected for snow retrievals such that *Tb* is

[1]Department of Geography, University of Waterloo, Ontario, Canada, N2L 2W1
[2]Hydrospheric and Biospheric Sciences Laboratory, NASA/Goddard Space Flight Center, Greenbelt, MD 20771, USA

directly related to surface features e_s and T_s (Chang et al., 1996). Two potentially interesting issues arise from this characterization and interpretation of the microwave emission from snow accumulation surfaces. First, it is known that the emissivity of snow is controlled by the characteristic dielectric properties of snow, especially grain size, snow density (volumetric fraction of grains) and the presence of liquid water content. These properties change as the snowpack undergoes metamorphosis which is a product of the thermal gradient through the pack (Kelly et al,. 2003). Second, Markus et al. (2006) found that atmospheric effects can affect the emission from snow on land and sea ice at high latitude, thus questioning the often-applied premise that the atmospheric components of (1) can be neglected. This paper explores the variations in microwave brightness temperatures over the Cold Lands Processes (CLPX) study site during the winter of the CLPX experiment in the winter of 2002-2003 and attempts to interpret those variations using *in situ* measurements of snow and atmospheric conditions. Not all field data collected during the CLPX experiment in February and March 2003 extend temporally over the entire winter season. Thus, a mixture of CLPX data and non-CLPX data are used in the analysis along with satellite passive microwave observations form the Advanced Microwave Scanning Radiometer – EOS (AMSR-E) instrument.

STUDY REGION

The study region used in this analysis is the CLPX domain in Colorado, USA. Figure 1 shows the regional study area along with the three mesoscale study areas (MSA) of North Park, Rabbit Ears and Fraser. The MSAs were 25 x 25 km in size with each one containing three 1x1 km intensive study areas (ISAs) in which intensive snow survey measurements were conducted between 19 and 25 February 2003 and between 26 and 30 March 2003.

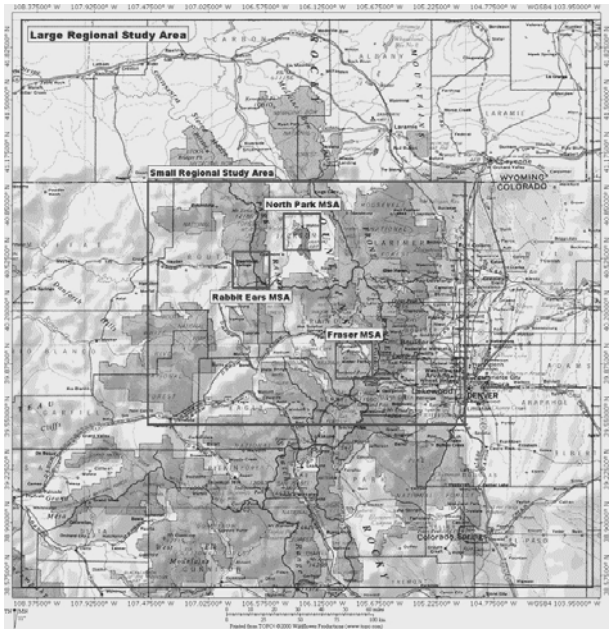

Figure 1. CLPX Study domain.

The North Park MSA is characterized as a low relief terrain with windswept snow cover that has small snow accumulation and, therefore, was not used in the analysis. The Rabbit Ears MSA is a moderately coniferous site with moderate to deep snow accumulation. The Fraser MSA is has moderate to high density coniferous stands with flat, steep and alpine terrain. Snow accumulation in the Fraser MSA is moderate. The Fraser MSA domain is used in this analysis.

DATA AND DATA ANALYSIS

AMSR-E Brightness Temperatures

AMSR-E was launched in 2002 aboard the Aqua satellite. It is a 6 frequency dual polarization instrument. Table 1 summarizes its characteristics with the Instantaneous Field of View (IFOV) representing the elliptical footprint samples on the ground within the swath. The central frequencies that are useful for estimating snow water equivalent (SWE) are generally considered the 18.7 and 36.5 GHz channels (hereafter referred to as 18 and 36 GHz) with the 36 GHz channel responsive to snow scattering and the 18 GHz channel responsive to the underlying surface temperature condition. More recently, the 10 GHz is also used since it has been suggested that the 18 GHz channel can be attenuated by deep snow.

Table 1 AMSR-E sensor characteristics.

Center Freq (GHz)	6.9	10.7	18.7	23.8	36.5	89.0
Band Width (MHz)	350	100	200	400	1000	3000
Sensitivity (K)	0.3	0.6	0.6	0.6	0.6	1.1
IFOV (km x km)	76 x 44	49 x 28	28 x 16	31 x 18	14 x 8	6 x 4

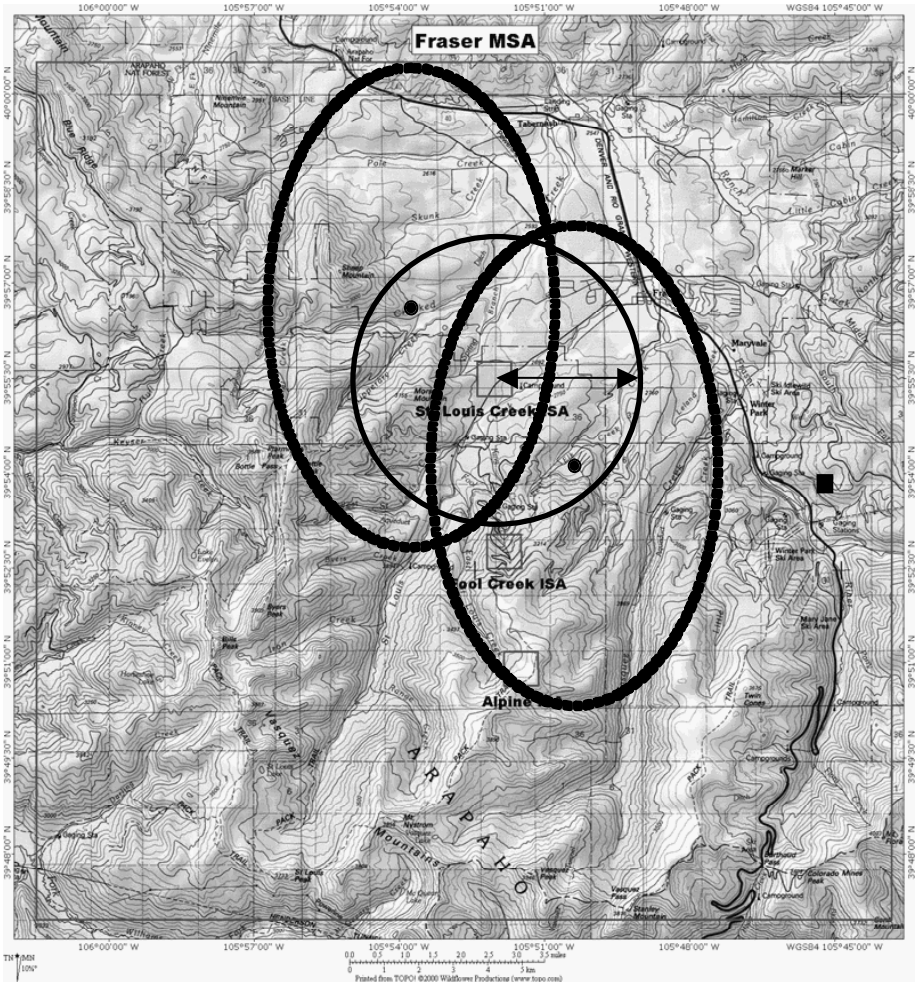

Figure 2. Fraser MSA with the ~4km radius (arrow) catchment area (black solid circle) used to collect AMSR-E 10, 18 and 36 GHz observations. The dotted ellipses illustrate the IFOV for two hypothetical 36 GHz IFOVs with the black dots representing the centres of the IFOVs. The square shows the approximate location of the nearest SNOTEL site at Arrow.

AMSR-E observations were obtained from nighttime passes from 1 November 2002 to 31 May 2003. Within each of the 25 x 25 km MSAs there were three 1x1 km ISAs. AMSR-E Tb data for Fraser MSA were extracted from the archive centring on St. Louis Creek and Fool Creek ISAs.

These ISAs represent locations in the MSA where snow cover is usually 100% throughout the main part of the winter accumulation season. Any AMSR-E (native resolution) IFOV with a centre of footprint location less than 0.04° of latitude or longitude (about 4km) from the centre of the ISAs was selected for the analysis. Figure 2 shows the locations of the three ISAs (square boxes) for the Fraser MSA and demonstrates the catchment area (4km radius) around the St. Louis Creek ISA used to select AMSR-E footprints; two IFOV footprint examples for the 36 GHz chennel are shown by way of an example (dotted ellipses with their centres of footprints identified as a black dot). The IFOV dimensions of the 18 and 10 GHz channel are not shown but would approximate the MSA extent (18 GHz) and extend further (10 GHz).

Time series of Tbs at 10, 18 and 36 GHz (vertical polarization) centred on St. Louis Creek and Fool Creek are shown in Figure 3a and 3b respectively. The series demonstrate that 10 and 18 GHz Tbs are similar in character throughout the season with both variations constrained to within a 10-15K range over several time periods. This in itself is interesting since most SWE retrieval algorithms rely on the lower frequency Tb (18 GHz) as a sub-nivean reference value against which the snow scattering scattering Tb channel (i.e. 36 GHz) is compared. Changes in the subnivean temperatures should be minimal since the snow is an efficient thermal insulator for snow-ground interface physical temperatures and the emissivity of the ground-snow interface should vary only slowly at the start of the season and at the end when melt-refreeze processes occur. The time series of the 36 GHz Tbs are similar to the 10 and 19 GHz Tbs except that the range in Tb variations are greater (30-40K). It is the short-term variations (1-3 weeks) that are of interest because in retrieval terms, they produce SWE estimates that are often not matched by measurements on the ground.

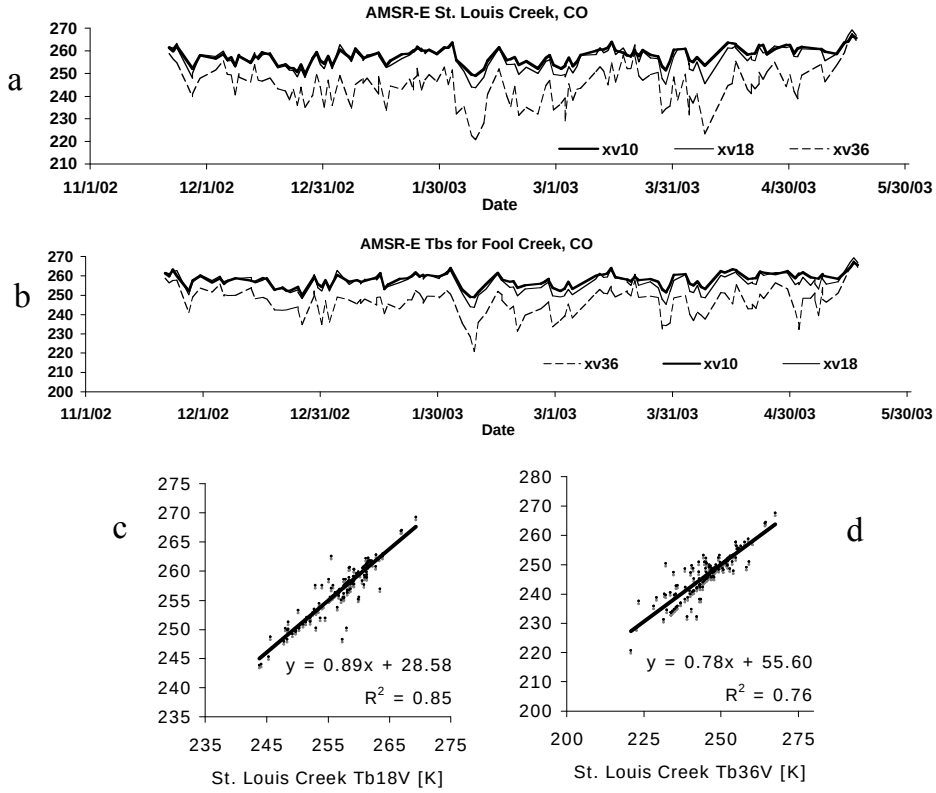

Figure 3. Tb time series for St. Louis Creek (a) and Fool Creek (b) for the CLPX winter season. Scatterplots of Tbs at 18 GHz (c) and 36 GHz (d) between St. Louis Creek and Fool Creek are also shown (see text for explanation).

The two ISAs, St. Louis Creek and Fool Creek are relatively close in the catchment. While snow accumulation in Fool Creek tends to be greater than at St. Louis Creek, both sites are tree-covered. The AMSR-E measured microwave emission at 10 and 18 GHz from both sites should be very similar given the fact that the footprints are large at these frequencies. Figure 3c shows a scatterplot of paired daily Tbs between Fool Creek and St. Louis Creek at 18 GHz for the 2002-2003 season. The R correlation is 0.92 suggesting high spatial consistency at this frequency for these sites. Figure 3d shows a similar scatterplot but for the 36 GHz channel data. The R correlation is 0.87 which is less than at 19 GHz. The IFOVs are is smaller at 36 GHz and therefore overlap is less. These figures suggest that there is spatial consistency between these sites.

Ground Data

To determine what the snow conditions on the ground were like during the CLPX season, *in situ* field measurement data were obtained from a combination of CLPX intensive study period field measurements, meteorological station measurements and Snotel data. Figure 4 shows a time series of snow depth measurements made by acoustic gauges on meteorological towers located at the centre of the St. Louis Creek and Fool Creek ISAs. The Figure shows that at both sites the snow accumulation was similar in character with the Fool Creek snow depth about 50% greater than the St. Louis Creek depth. A probable anomalous period is shown in the Fool Creek data for the first two weeks in February when there is almost a doubling of the snow depth record. This is likely to be caused by instrument error which appears to be resolved by the middle of February. Since the St. Louis Creek site is les than 5 km away and does not show this short duration elevated snow depth, it is unlikely that the Fool Creek data are correct for this short period.

The snow depth record exhibits a gradual increase in snow depth to mid march when there is a large snowfall event before a gradual decrease in snow depth to the middle of June. There are also short time-scale variations of snow depths that punctuate the general trend with fluctuations of a few centimeters depth over a few days.

Continuous snow water equivalent was not measured at either of these sites. However, it was measured at the Arrow SNOTEL site (see Figure 2 for location). Figure 5 shows the characteristic SWE variation during CLPX and it clearly demonstrates a gradual build-up over the period with no rapid variations of the kind found in Figure 4. Snow depth changes with new snow accumulation, sublimation and snow densification processes and the time variation is often characterized by a saw-tooth pattern. SWE, however, is a more continuous accumulation process since changes to SWE are from sublimation or melt, both of which are, generally, longer-term processes. While it is tempting to relate the short-term fluctuations of 36 GHz Tbs in Figure 3 to snow depth changes, variations in SWE (the variable more closely related to Tb at 36GHz) suggest that changes in bulk SWE properties do not significantly contribute to changes in Tbs in Figure 3.

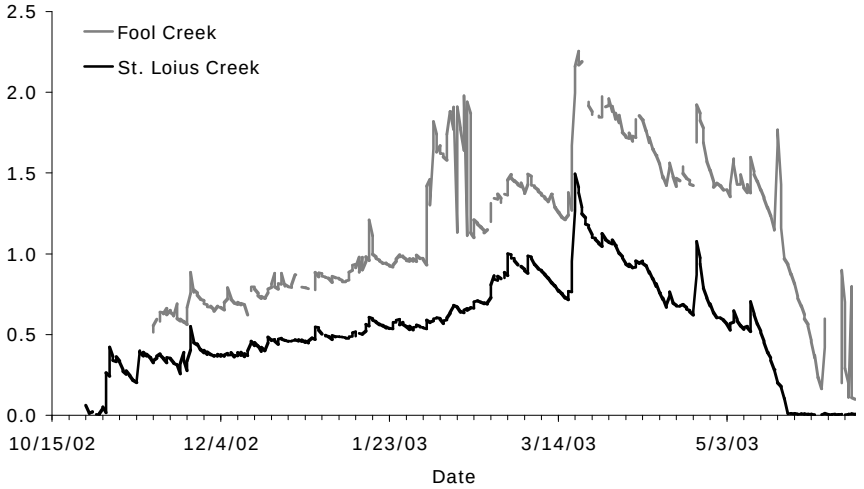

Figure 4. Snow depth at 00:00 and 12:00 hrs from acoustic gauges at Fool Creek and St. Louis Creek ISAs.

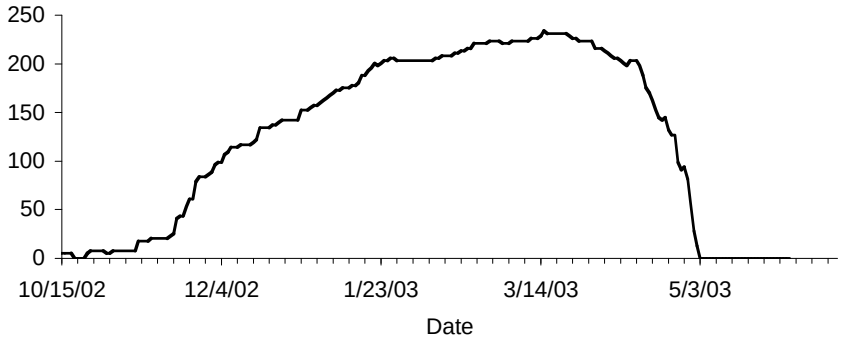

Figure 5. Snow water equivalent from the Arrow SNOTEL site (39° 54'N, 105° 45'W).

To assess whether the Tb variations in the passive microwave response were related to internal snowpack properties, density and grain size statistics from each CLPX ISA for the third intensive observation period (IOP-3) (19-26 February, 2003) and IOP-4 (25-31 March, 2003. Both variables can strongly influence the microwave response from snow especially snow grain size. Although daily measurements of these two variables were not made during the season for any ISA, measurements made during the discrete IOP periods allow a cursory assessment of the magnitude of seasonal change in these two variables, especially between IOPs in the same winter season (*i.e.* IOP-1 to IOP-2 and IOP-3 to IOP-4). Figure 6 shows the mean (bar) and standard deviation (error bars) of grain size and density for Fool Creek and St Louis Creek during each of the IOPs (including the 2002 IOP-1 and IOP-2). From IOP1 to IOP2 and from IOP3 to IOP4, the grain size at Fool Creek was remarkably constant for each of the small, medium and large grain size samples (a, b and c). At St. Louis Creek, the grain sizes for each of these small, medium and large populations was also relatively constant between IOP1 and IOP2 and between IOP3 and IOP4. This suggests that grain size, did not change significantly between middle and end of snow seasons for both 2002 and 2003.

Figure 6d shows density statistics for the same sites. Snow pit mean density values changed relatively little from IOP-3 to IOP4 and alos between IOP-1 and IOP-2. Between IOP3 and IOP4 at St. Louis Creek, mean density also did not change substantially. Between IOP1 and IOP2, mean snow density at St. Louis Creek increased. However, given the consistency in the other sites, and that mean snow density tends to change slowly, it is unlikely that changes in density contribute to the magnitude of changes observed in the microwave Tbs.

Last, ambient air temperature measurements were taken from the ISA meteorological observing stations during the CLPX winter of 2002-2003. Figure 7 shows the time series of air temperature above the snow and at the snow-ground interface every hour for Fool Creek and St. Louis Creek for the 2002-2003 winter season (IOP-3 and IOP-4). The data for both sites are very similar. The snow-ground interface temperature at both ISAs shows very little variability once the snow begins to accumulate (1 November, 2002) until the end of the snow season when it melts off (about 18 May for St. Louis Creek and 1 June for Fool Creek). The air temperature variations are also comparable between ISAs with nearly matching magnitude and timing of the peaks and troughs. Consistency between sites is strong suggesting that air temperature variations at both sites were similarly dynamic not only at the diurnal scale but also at the inter-diurnal scale. The air temperature records suggest that of all the data sets assessed, the greatest temporal variability was found in this state variable. Furthermore, when compared with the brightness temperatures at 18 and 36 GHz (vertical polarization), there is a striking agreement between the air temperature and the Tbs. Figure 8 shows a comparison of air temperature with Tb36V and Tb18V for St. Louis Creek during the 2002-2003 CLPX season. The air temperature data were selected to coincide with the AMSR-E pass times.

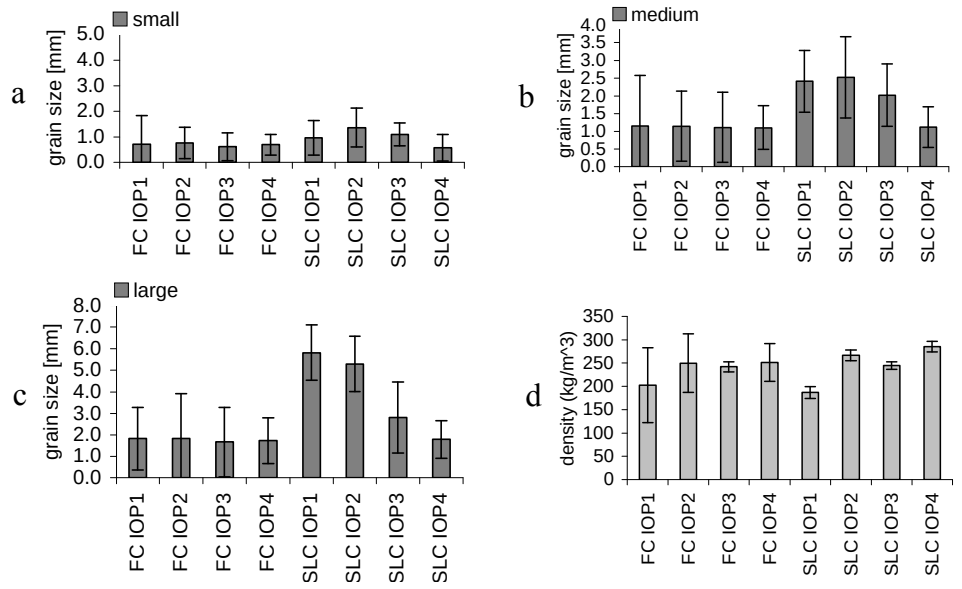

Figure 6. Mean small (a), medium (b) and large (c) grain size measurements from pit excavations at Fool Creek (FC) and St. Louis Creek (SLC) ISAs for the IOPS during CLPX. The bars represent the mean and the error bars the standard deviations. Figure 6d shows the average density at both ISAs during the different IPOS with the mean density shown by the bar and the standard deviation shown by the error bars.

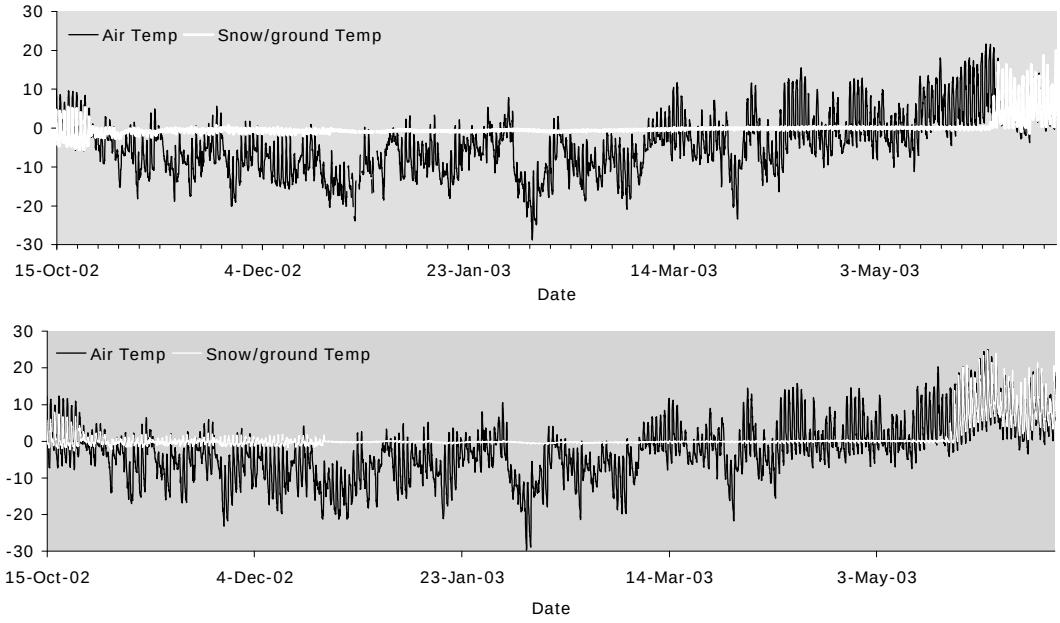

Figure 7. Air and snow-ground temperatures for Fool Creek (upper panel) and St. Louis Creek (lower panel) during the 2002-2003 CLPX winter season.

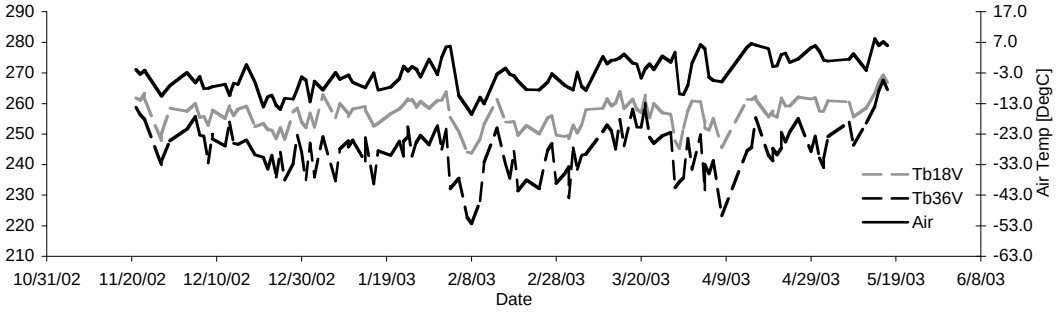

Figure 8. Comparison of air temperature with AMSR-E brightness temperatures at 18 and 36 GHz (Tb18V and Tb36V).

To further quantify the relationships a correlation analysis shows that air temperature is correlated with Tb18V and Tb36V with a correlation coefficient of 0.56 and 0.36 respectively (both significant at $p < 0.001$). The correlation coefficient increases to 0.67 at Tb10V.

SIGNIFICANCE AND CONCLUSIONS

Practical approaches developed to estimate SWE using passive microwave remote sensing instruments generally exploit wavelength-dependent brightness temperature characteristics of emitted radiation from a snowpack. In addition to the snowpack physical characteristics (grain size, density, SWE) retrieval schemes have attempted to parameterize *in situ* vegetation characteristics and underlying ground conditions which are known also to influence the microwave response from snow (Chang et al. 1996). Simple retrieval methods consider that for a snowpack with SWE greater than 10 mm, scattering processes by snow grains are significant in microwave emission from snow and can be detected at frequencies greater than about 25 GHz. The strength of scattering signal is determined by the brightness temperature difference between 18 and 36 GHz and is considered proportional to the SWE or snow depth thus forming the basis of a relationship for estimating SWE. For the CLPX domain, this study suggests that physical temperature (air temperature) affects the brightness temperature more strongly at the lower frequency channels (10 and 18 GHz) than at the higher frequency channels (36 GHz) and that the uneven contribution by the thermal signal to the two frequencies may be a key contributing factor causing the inter-diurnal variations in brightness temperature in any brightness temperature difference retrieval approach. Figure 9 shows the difference in Tb18V and Tb36V for the 2002-2003 CLPX study period. It suggests, qualitatively, that a proportion of the variation in the Tb18V-Tb36V line is in anti-phase with the air temperature curve. While a significant part of this brightness temperature difference is related to snowpack bulk properties (emissivity), there is a significant physical temperature component that is not removed by a frequency difference algorithm and is perhaps the reason for the observed fluctuations in the Tb18V-Tb36V curve. Further analysis is needed to quantify the contribution of the physical temperature to the brightness temperature of a snowpack at multiple frequencies so that it can be better removed from the SWE retrieval process.

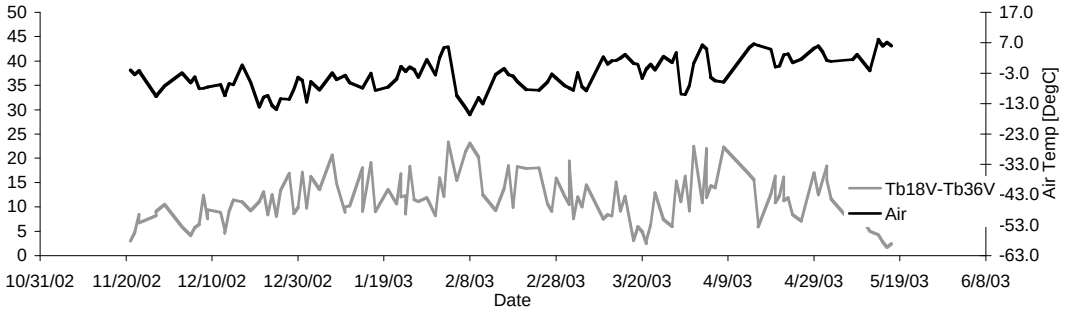

Figure 9. Time series of air temperature and brightness temperature difference between Tb18V and Tb36V for the 2002-2003 CLPX period.

REFERENCES

Chang ATC, Foster JL, Hall DK. 1996. Effects of forest on the snow parameters derived from microwave measurements during the Boreas winter field campaigns, *Hydrological Processes* **10**: 1565-1574.

Kelly REJ, Chang ATC, Tsang L, Foster JL. 2003. Development of a prototype AMSR-E global snow area and snow volume algorithm, *IEEE Transactions on Geoscience and Remote Sensing*, **41**: 230-242.

Markus T, Powell DC, Wang JR. 2006. Sensitivity of passive microwave snow depth retrievals to weather effects and snow evolution, *IEEE Transactions on Geoscience and Remote Sensing* **44**: 68-77.